Cerberus is a head-inducing secreted factor expressed in the anterior endoderm of Spemann's organizer

Tewis Bouwmeester, Sung-Hyun Kim, Yoshiki Sasai, Bin Lu & Eddy M. De Robertis

Howard Hughes Medical Institute and Department of Biological Chemistry, University of California, Los Angeles, California 90095–1737, USA

An abundant cDNA enriched in Spemann's organizer, *cerberus*, was isolated by differential screening. It encodes a secreted protein that is expressed in the anterior endomesoderm. Microinjection of *cerberus* mRNA into *Xenopus* embryos induces ectopic heads, and duplicated hearts and livers. The results suggest a role for a molecule expressed in the anterior endoderm in the induction of head structures in the vertebrate embryo.

THE organizer experiment[1] demonstrated that the dorsal lip of the amphibian gastrula has, when transplanted, the ability to recruit or organize neighbouring cells to form a twinned body axis. The grafted tissue has potent inducing activities, leading to the formation of a secondary central nervous system, dorsal mesodermal tissues, such as somites, and a secondary gut. Interest in the multiple activities of the organizer has led to the isolation of many genes expressed specifically in the dorsal lip of the *Xenopus* gastrula. Their products include nuclear proteins, mostly homeodomain proteins, such as goosecoid[2], Xlim-1 (ref. 3), XFKH1/pintallavis[4,5], Xnot[6], Xnot-2 (ref. 7), Siamois[8], Otx2 (refs 9, 10) and Xanf-1 (ref. 11), and secreted proteins such as noggin[12], follistatin[13], chordin[14,15] and members of the transforming growth factor (TGF)-β family of growth factors[16–18]. *In situ* hybridization studies suggest that the organizer consists of multiple overlapping domains defined by these gene markers[16,19], and the task of mutating each of the mouse homologues of these organizer-specific genes, to analyse how they interact with each other, is under way[20].

The organizer region leads not only to the induction of multiple tissue types, but also to the development of anteroposterior polarity. Spemann recognized that early dorsal lips could induce entire axes, including head structures, but older dorsal lips would lose the ability to induce head, leading only to the formation of trunk–tail structures[21]. Studies in the mouse have provided genetic evidence for the existence of a head organizer region. Inactivation of *Lim-1* leads to mice lacking all head structures anterior to rhombomere 3, but having normal trunk–tail structures[22]. Mutations of murine *Otx2* and, to some extent, *HNF3β* also cause severe deletions anterior to rhombomere 3 (refs 20, 23). In *Xenopus*, several experimental treatments can lead to the formation of normal trunk–tail structures lacking structures anterior to the hindbrain[24–26]. It seems that the formation of the anterior head region, where *Hox* genes are not expressed, is regulated differently from the hindbrain and trunk-tail region.

To explore further the molecular complexity of Spemann's organizer, we performed a differential screen for dorsal-specific cDNAs. The second most abundant mRNA found in the dorsal region of the *Xenopus* gastrula encodes a novel putative secreted protein designated cerberus. The *cerberus* mRNA has potent inducing activity in *Xenopus* embryos, leading to the formation of ectopic heads. Unlike other organizer-specific factors[12–17], *cerberus* does not modify the fate of mesoderm, but instead suppresses the formation of trunk–tail mesoderm. It defines an anterior dorsolateral domain of the gastrula, including the leading edge of the deep layer of the dorsal lip, a region that, as shown here, gives rise to foregut and midgut endoderm. It also promotes the formation of cement gland, olfactory placodes, cyclopic eyes, forebrain and duplicated heart and liver (a foregut derivative). The expression pattern and inducing activities of *cerberus* suggest an important role for a factor expressed in prospective foregut endoderm in the induction of the head region of the embryo.

A putative secreted protein encoded by *cerberus*

A differential screening approach was used to identify abundant dorsal-specific cDNAs without bias as to their function. As shown in Table 1, five previously known and five new cDNAs were isolated. The most abundant dorsal-specific cDNA was *chordin* (*chd*), with 70 independent isolates; the second most abundant cDNA was isolated 11 times, and was named *cerberus* (after a mythological guardian dog with multiple heads). The *cerberus* cDNA encodes a polypeptide of 270 amino acids, with an amino-terminal hydrophobic signal sequence and a carboxy-terminal cysteine-rich region (Fig. 1*a*). Preliminary experiments indicate that the cerberus protein is secreted into the culture medium of mRNA-injected *Xenopus* oocytes (T.B., unpublished observations). The amino-acid sequence of cerberus and the spacing of its nine cysteine residues were not significantly similar to other proteins in the databases (NCBI-Gen Bank release 93.0). We conclude that *cerberus* is an abundant dorsal-specific cDNA that encodes a novel secreted protein.

Demarcation of an anterior organizer domain

The *cerberus* mRNA is expressed at low levels in the unfertilized egg, and zygotic transcripts increase at stage 10 (Fig. 1*b*). Expression continues during gastrula and early neurula, rapidly declining during neurulation. Importantly, zygotic transcripts of *cerberus* accumulate about one hour later than those of *chd*, suggesting that *cerberus* could act downstream of the *chd* signal (Fig. 1*b*).

Whole-mount *in situ* hybridizations[27] show that *cerberus* zygotic expression becomes detectable in the yolky endomesodermal cells located in the deep layer of the organizer, in a domain that includes the leading edge of the most anterior cells and extends into the dorsal half of the floor of the blastocoel at stage $10\frac{1}{2}$ (Fig. 2*a–c*). In sections, *cerberus* mRNA is found in the deep yolky cells (Fig. 2*b*), which by stage $10\frac{1}{2}$ are separated from the neuroectoderm by a virtual space, called Albert Brachet's cleft (Fig. 2*b*, *k*), which in *Xenopus* forms long before the bottle cells of the external blastopore lip start ingressing[28–30]. Expression of *cerberus*

a

```
MLLNVLRICI IVCLVNDGAG KHSEGRERTK TYSLNSRGYF   40
RKERGARRSK ILLVNTKGLD EPHIGHGDFG LVAELFDSTR   80
THTNRKEPDM NKVKLFSTVA HGNKSARRKA YNGSRRNIFS  120
RRSFDKRNTE VTEKPGAKMF WNNFLVKMNG APQNTSHGSK  160
AQEIMKEACK TLPFTQNIVH ENCDRMVIQN NLCFGKCISL  200
HVPNQQDRRN TCSHCLPSKF TLNHLTLNCT GSKNVVKVVM  240
MVEECTCEAH KSNFHQTAQF NMDTSTTLHH             270
```

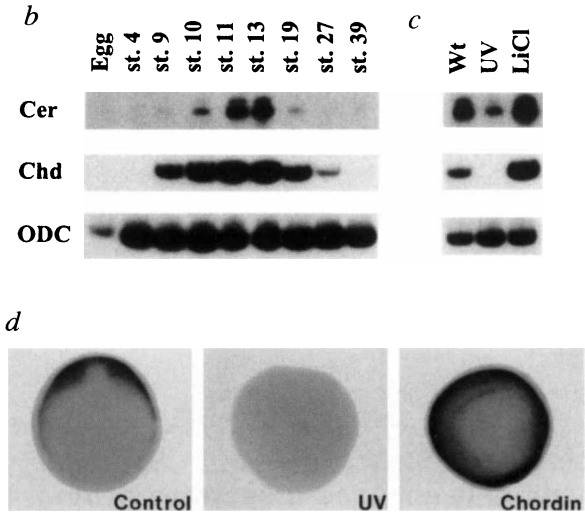

FIG. 1 *Xenopus cerberus* encodes a putative secreted protein transiently expressed during embryogenesis. *a*, Deduced amino-acid sequence of *Xenopus* cerberus protein. The signal peptide sequence and the 9 cysteine residues in the C terminus are in bold. Potential N-linked glycosylation sites are underlined. In a BLAST database search, cerberus showed limited similarity only to the mammalian Dan protein, a possible tumour suppressor proposed to be a DNA-binding protein[47]. However, the spacing of the cysteine residues and a crucial histidine in the proposed Dan zinc-finger domain are not conserved, indicating that the weak conservations identified by the computer might not be significant. *b*, Temporal expression of *cerberus*. Total RNA, isolated from the indicated stage (st.) of development, was analysed by RT–PCR for levels of expression of *cerberus* (Cer), *chordin* (Chd) and *ornithine decarboxylase* (ODC), which serves as a loading control. Zygotic expression of *cerberus* starts 1 h after *chd* activation, and is transiently expressed during gastrulation and neurulation. Expression of *cerberus* can be observed in unfertilized egg and blastula stages at low levels in longer exposures. *c*, RNAs from control (Wt), ultraviolet (UV)- or LiCl-treated embryos analysed by RT–PCR at stage 11. The relative intensity differences with *b* are due to differences in exposure time. *d*, *In situ* hybridization of wild-type controls, UV-treated and *chordin*-injected stage-11 embryos hybridized with *cer* antisense RNA.

METHODS. RNA was isolated from the indicated stages of development with the RNA STAT kit (Tel-Test). Quantitative RT–PCR and primers were as ref. 15, except: *cer* (forward primer (F), 5′-GCTGAACTATTTGATTCCACC; reverse primer (R), 5′-ATGGCTTGTATTCTGTGGGGC; 28 cycles); *chd* (F, 5′-CCTCCAATCCAAGACTCCAGCAG; R, 5′-GGAGGAGGAGGAGCTTTGGGACAAG; 28 cycles); *ODC* (accession no. X56316) (F, 5′-GTCAATGATGGAGTGTATG-GATC; R, 5′-TCCATTCCGCTCTCCTGAGCAC; 28 cycles). UV and LiCl treatment were as described[14]. Whole-mount procedure is described in Fig. 2.

(Fig. 2*b*, *c*) does not extend into the dorsal lip, which is marked by *chd*, although an area of overlap can be seen in histological sections (Fig. 2*b*). At mid-gastrula (stage 11), *cerberus* expression is suppressed in the dorsal midline in a region that appears to correspond to prechordal plate precursor cells (Fig. 2*d*). To substantiate this observation we compared the expression domains of *cerberus* (dorso-anterior yolky endomesoderm), *Xbra* (ref. 31; trunk–tail mesoderm), *Xlim-1* (ref. 3; prechordal and notochordal precursors), *goosecoid* (ref. 2; prechordal plate), *Xnot-2* (ref. 7; notochord) and *chd* (ref. 14; prechordal and notochordal cells) in a double-labelled *in situ* hybridization study. The *cerberus* midline gap does not correspond to notochordal tissue because *Xbra* and *Xnot-2* do not overlap with it (Fig. 2*d*, *h*). Conversely, this gap coincides with markers expressed in prechordal plate precursors such as *Xlim-1* (Fig. 2*e*), *goosecoid* (Fig. 2*f*, *g*) and *chd* (Fig. 2*i*). The patterns are highly dynamic; for example, at early gastrula, *goosecoid* and *Xlim-1* extend to the floor of the blastocoel, overlapping extensively with *cerberus* (not shown), whereas at mid-gastrula they separate from each other, so that *cerberus* occupies the anteriormost endomesoderm (Fig. 2*c*), and *goosecoid* and *Xlim-1* become restricted to prospective prechordal plate (Fig. 2*g* and data not shown). Within the mid-gastrula stage there are subtle differences in expression domains. We note that *Xlim-1* and *chd* have wider domains than *goosecoid* (Fig. 2*e*, *f*, *i*), resulting in areas of overlap with *cerberus*-expressing cells in the lateral margins. At early neurula (stage 13), *cerberus* mRNA is found in a broad anterior domain of endomesoderm that excludes the prechordal plate before becoming undetectable by stage 14 (not shown).

As summarized in Fig. 2*j*, these comparative *in situ* hybridization studies show that the endomesoderm of the dorsal side of the gastrula can be subdivided into three main regions: (1) the future trunk–tail mesoderm defined by *Xbra*; (2) the prospective prechordal plate that expresses *chd*, *goosecoid* and *Xlim-1*; and (3) a broad anterior domain of *cerberus*-expressing cells that includes the leading edge of the gastrulating endomesoderm.

To investigate whether *cerberus* expression is controlled similarly to Spemann's organizer activity, we analysed its expression in ultraviolet-treated embryos. This treatment (Fig. 1*c*, *d*), which prevents the induction of Spemann's organizer[24], was found to inhibit *cerberus* strongly. Conversely, when the amount of Spemann's organizer is increased by treatment with LiCl[24], *cerberus*, like *chd*, is upregulated (Fig. 1*c*). We therefore tested whether *cerberus* can be activated by signals secreted by the organizer. Embryos were injected into each of the four blastomeres with *chd* (Fig. 1*d*), *noggin* or *follistatin* (not shown) mRNAs, all of which expanded expression of *cerberus* radially in the endomesoderm. The results suggest that *cerberus* delineates a novel anterior domain of the *Xenopus* gastrula that is controlled in a similar way to Spemann's organizer.

Prospective foregut marked by *cerberus*

The population of *cerberus*-expressing cells at the leading edge of the gastrulating endomesoderm (Fig. 2*c*) has been poorly defined in *Xenopus*. Apart from experiments in which explants of this region gave rise to liver[32], little is known about the fate of these anteriormost gastrulating cells. We labelled the leading edge of these cells with the hydrophobic lineage tracer DiI (Fig. 2*k*) to determine their fate, and cultured the embryos until stage 30. In 85% of the cases ($n = 47$, two experiments) the lineage tracer marked the large endodermal cells of the foregut, particularly in the liver diverticulum, and the anterior midgut (Fig. 2*l*). Contrary to our expectations, we did not observe labelled cells in the prechordal plate, head mesoderm or pharyngeal endoderm. In hindsight, the fate of the leading-edge cells could have been predicted from detailed examination of published histological sections of *Xenopus* embryos[28,33]. Lateral to the midline, the *cerberus*-positive region becomes heart primordium[34]. We conclude from this cell-lineage study that the dorsal leading edge of the gastrula gives rise to foregut, liver and midgut.

Suppression of trunk–tail mesoderm formation

Microinjected *cerberus* mRNA has potent effects on *Xenopus* development. Radial injection of high doses (100 pg per blastomere) of *cerberus* mRNA into each blastomere of the four-cell embryo results in embryos with very large cement glands (Fig. 3*a*). These embryos do not form trunk–tail mesoderm, as indicated by the repression of *Xbra* (Fig. 3*b*), the lack of an external blastopore

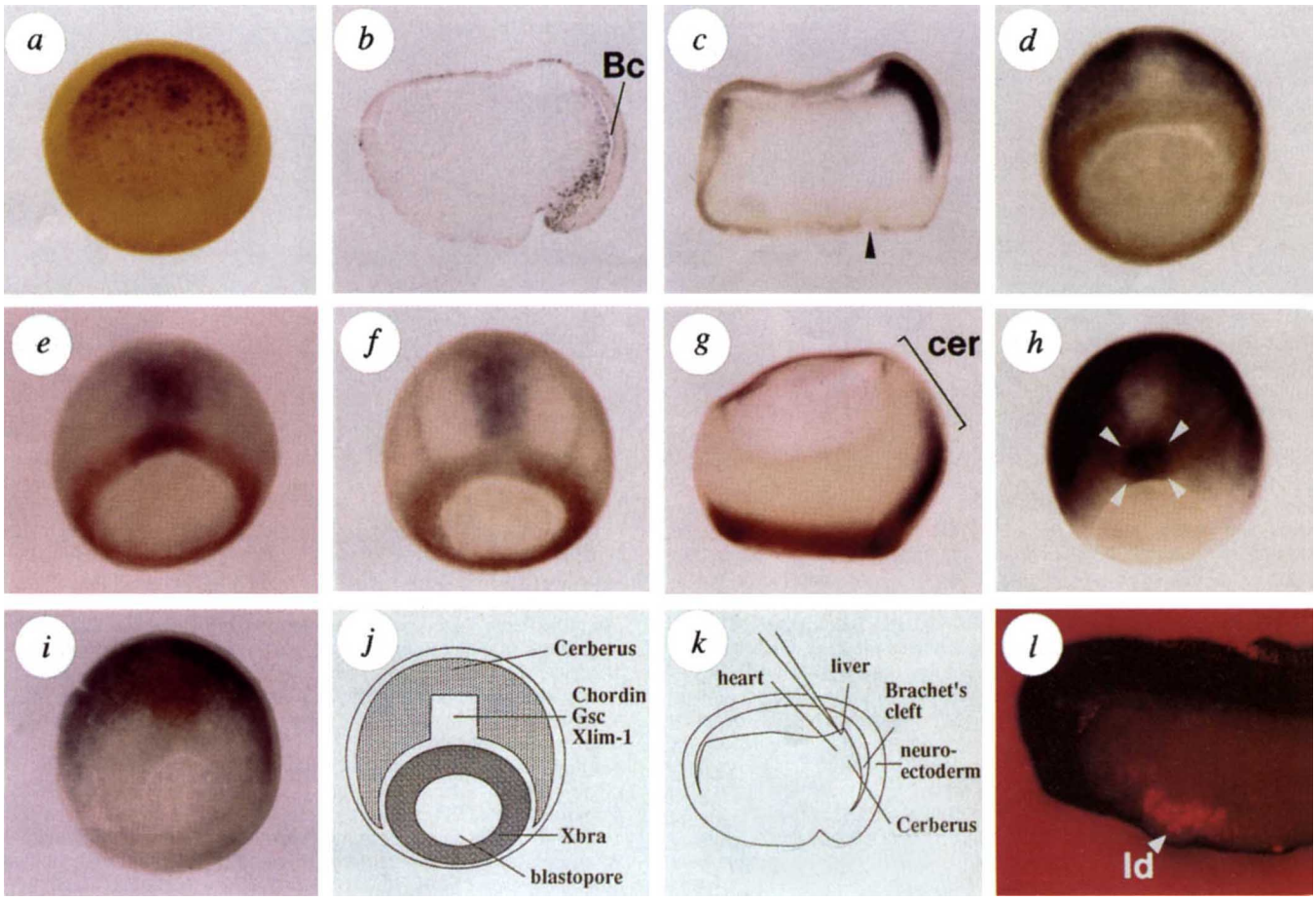

FIG. 2 The *cerberus* (*cer*) expression domain and comparison with other organizer genes. *a*, Top view at stage $10\frac{1}{2}$, showing *cer* expression in the dorsal half of the deep endomesodermal cells and the floor of the blastocoel. *b*, Histological section of a stage-$10\frac{1}{2}$ gastrula stained with *cer* (blue) and *chd* (brown); *chd* is expressed in the dorsal lip, *cer* in the anterior endomesoderm (separated from the neuroectoderm by Brachet's cleft, Bc). Note the overlap between the two areas of expression. *c*, Lateral view of *cer* at stage $10\frac{3}{4}$ marking the anteriormost endomesoderm. The *cer* domain does not extend to the blastopore (arrowhead). *d*, Double staining of mid-gastrula (stage 11) embryo for *cer* (blue) and *Xbra* (brown); *cer* expression is anterior to *Xbra*, which forms a ring defining the trunk–tail mesoderm region. Note that *cer* expression is suppressed in the midline region corresponding to the future prechordal plate. *e*, Double staining (stage 11) for *Xlim-1* (blue) and *Xbra* (brown). *f*, Comparison of *gsc* (blue) and *Xbra* (brown), dorsal view. *g*, Lateral view of *goosecoid* (*gsc*) and *Xbra* double labelling. At stage 11, *gsc* (blue) does not reach the leading edge. The region corresponding to *cerberus* expression in the anteriormost endomesoderm is indicated. *h*, Comparison of *cer* and *Xnot-2*, both blue. Arrowheads mark *Xnot-2* notochordal expression. The prechordal plate gap is not stained. *i*, Double staining (stage $11\frac{1}{2}$) for *cer* (blue) and *chd* (brown) showing that *chd*, which marks the prechordal plate at this stage, occupies the *cer* gaps and overlaps with *cer* in lateral regions. *j*, Schematic representation of a mid-gastrula embryo showing the three main subdivisions of the dorsal side of the *Xenopus* endomesoderm suggested by comparative double-labelling studies. The anterior endomesoderm expresses *cer*; the prechordal plate region expresses *chd*, *gsc* and *Xlim-1*; the trunk–tail mesoderm expresses *Xbra*. *k*, Design of lineage tracing experiment. Schematic diagram showing a lateral view of an early gastrula indicating the injection of the DiI tracer through a cut in the animal cap; *cerberus* is expressed in cells fated to become liver and cardiac primordia. *l*, Side view of a tailbud embryo (stage 30), with anterior to the left, showing labelling in the descendants of the injected leading-edge cells. Fluorescent cells can be identified as endodermal owing to their large size, and are located in the foregut, liver diverticulum (ld) and anterior midgut.

METHODS. Whole-mount *in situ* hybridization was performed as described[14,27], using a pBS-*cer* plasmid containing a 1.4-kb insert linearized with *Eco*RI and transcribed with T7 RNA polymerase. Double-labelling procedure was as described[48]; *cer*, *Xlim-1* (ref. 3), *gsc* (ref. 2) and *Xnot-2* (ref. 7) were labelled with digoxigenin-UTP, whereas *chd*[14] and *Xbra*[31] probes were labelled with fluorescein-UTP. DiI labelling[7] was done by injecting the dye through a cut in the blastocoel roof (which heals rapidly) into the midline of the leading edge of the crawling endomesodermal yolky cells of stage-$10\frac{3}{4}$ embryos. Lineage-traced embryos were incubated in the dark until stage 30, fixed and photographed[7].

lip, even at stage 13 (Fig. 3*c*), and by several molecular markers (Fig. 3*h*).

Radial injection of *cerberus* mRNA also affects prechordal plate mesoderm. This is reflected in the appearance of cyclopic eyes, particularly in embryos injected radially with low doses (20 pg) of *cerberus* mRNA (Fig. 3*d*). During amphibian development, the prospective eye region is initially specified as a single field that is subsequently split into two eye primordia by signals emanating from the prechordal plate[35]. Thus *cerberus*, a gene not expressed in the prechordal plate (Fig. 2*j*), seems to repress prechordal plate function when misexpressed; this view is supported by the ability of *cerberus* to suppress *goosecoid* expression in *in situ* hybridizations at the early neurula stage (data not shown).

Axial development can be restored in embryos ventralized by ultraviolet treatment by several organizer-specific genes[8,12,14,17,26]. However, microinjection of *cerberus* mRNA into single blastomeres of eight-cell ultraviolet-treated embryos did not lead to the rescue of trunk–tail axial structures; instead it promoted formation of a large endodermal mass and a smaller head-like structure containing single cement glands and, at later stages, a small cyclopic eye (Fig. 3*e*, *f*). To eliminate the possibility that this phenotype could be due to an overdorsalization of the embryo, we performed concentration curves (20, 40 and 80 pg per embryo, $n = 40$), and found no evidence of trunk–tail structures, even at the lowest mRNA concentration (in which only cement glands were observed); this interpretation was supported by molecular analysis (not shown). Histological analysis of the head-like structures revealed the presence of differentiated brain tissue, recog-

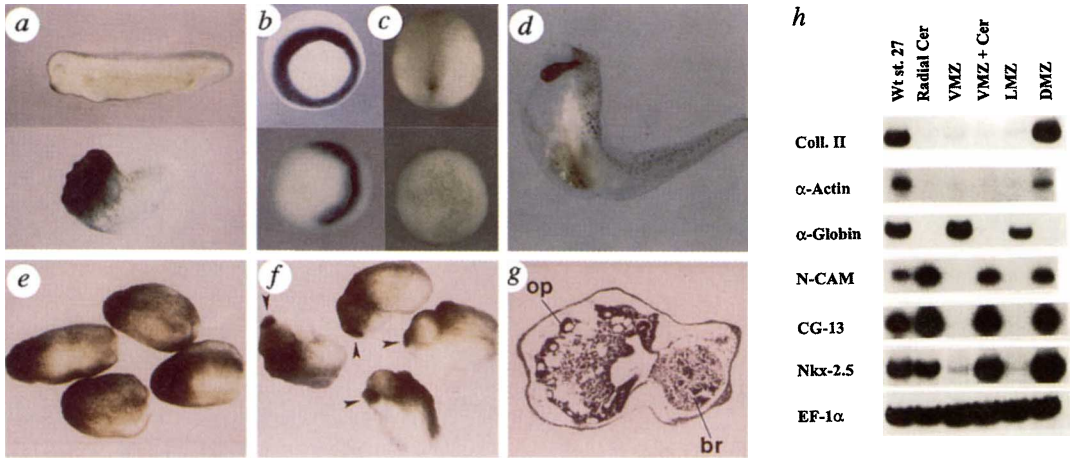

FIG. 3 Injection of *cerberus* mRNA into 4-cell embryos suppresses axial mesodermal structures and induces anterior neural structures in UV-ventralized embryos. *a*, Control stage 27 (top), and embryo injected radially into each blastomere at the 4-cell stage with 100 pg pBS-*cer* mRNA (bottom), showing presence of pronounced cement gland and absence of axial trunk–tail structures. *b*, Expression of *Xbra* in control stage 11 (top) and in an embryo injected laterally with *cerberus* mRNA (bottom). Note that *cerberus* suppresses *Xbra* and blastopore lip formation in half the embryo. *c*, Control stage 13 (top) and vegetal view of a radially *cer*-injected sibling lacking the blastopore (bottom). *d*, Embryo injected radially with low (20 pg per blastomere) pBS-*cer* mRNA, leading to formation of a cyclopic eye. *e*, UV-control embryos showing complete ventralization. *f*, UV-injected embryos (single injection of 40 pg pBS-*cer* mRNA at the 8-cell stage, $n = 20$) showing induction of small head-like structures containing cement glands (arrowheads). No rescue of axial structures was observed at lower or higher doses. *g*, Histological section through a UV *cerberus* injected embryo indicating the brain (br) and morphologically recognizable dense olfactory placodes (op); (see Fig. 5*c* top inset for normal olfactory placode). *h*, Molecular analysis by RT–PCR for expression of gene markers in radially injected embryos and in VMZ-injected explants. Controls (Wt, stage 27), VMZ, LMZ (explants devoid of organizer tissue) and DMZ are controls (see text). Expression of mesodermal (*collagen II*, *α-actin*, α-globin), cardiac (*Nkx-2.5*), neural (*N-CAM*) and cement gland (*CG-13*) gene markers were analysed. *EF-1α* is a loading control.

METHODS. Capped synthetic mRNA was produced form two sources: pBS-*cer* (original isolate in pBluescript SK$^-$ linearized with *Xho*I, transcribed with T3) or pSP35-*cer* (construct with β-globin 5′ and 3′ flanking sequences[40], linearized with *Not*1 and transcribed with SP6) using the Ambion Message Machine kit. To construct pSP35-*cer*, the coding region of *cerberus* was amplified by PCR using the following oligos: (F, 5′-ACGGAATTCACAATGTTACTAAATGTACTCAGG and R, 5′-TGCGTCGACTTAATGGTGCAGGGTAGTAGATGT), and cloned into the *Eco*RI and *Sal*I sites of pSP35 (ref. 40). Radial injections were performed in the equator region of each blastomere of a 4-cell embryo, at concentrations ranging from 100 to 10 ng μl^{-1} RNA synthesized from both pBS-*cer* and pSP35-*cer*. Similar results were obtained with both mRNAs, except that pSP35-*cer* was as active at lower dilutions (about 2 times). Control injections of pBS-Δ*cer* (in which a small deletion was introduced between nucleotides 346 and 566 and that results in a frameshift) had no phenotypic effect in these and other assays. Cyclopic phenotypes were also obtained with a pCS2-*cer* (CMV promoter-driven) DNA construct (not shown). UV embryos were obtained as described[14] and injected into a single vegetal blastomere at the 8-cell stage. Primer sets for RT–PCR were previously described[15] except for the following new sets: *Nkx-2.5* (F, 5′-GAGCTACAGTTGGGTGTGTGTGGT and R, 5′-GTGAAGCGACTAGGTATGTGTTCA; 28 cycles[34]); *Edd* (F, 5′-TATTCTGACTCCTGAAGGTG, and R, 5′-GAGAACTGCCCATGTGCCTC; 28 cycles[40]). Whole-mount *in situ* hybridization[27] was performed with antisense *Xbra* RNA[31].

nizable by the presence of grey and white matter and, connected to the brain, large masses of tissue with the histological appearance of multiple olfactory placodes (Fig. 3*g*; see Fig. 5*c* top inset for a normal *Xenopus* olfactory placode). Thus *cerberus* mRNA differs from previously described organizer factors in that it promotes formation of cement gland and anterior neural structures, but does not rescue axis formation in embryos ventralized by ultraviolet treatment.

To confirm that mesoderm formation is suppressed in radially injected embryos, and that *cerberus* mRNA is unable to dorsalize ventral mesoderm, we analysed several molecular markers by reverse transcription polymerase chain reaction (RT–PCR) analysis (Fig. 3*h*). RNAs from stage-27 uninjected embryos (Wt), ventral marginal zone (VMZ), lateral marginal zone (LMZ, lacking the organizer region) and dorsal marginal zone (DMZ) explants were used as controls. In radial injections, *cerberus* mRNA abolished the expression of notochordal (*collagen II*), somitic (*α-actin*) and ventral (*α-globin*) trunk mesoderm markers. In VMZ explants, *cerberus* mRNA did not cause dorsalization (that is, *collagen II* and *α-actin* were not induced) and repressed ventral mesoderm (*α-globin* was inhibited). Instead, in these VMZ explants *cerberus* induced the expression of neural (*N-CAM*), cement gland (*CG-13*) and heart primordium (*Nkx-2.5*) (ref. 34) markers.

These data indicate that *cerberus* has biological activities that differ from all other known organizer-specific genes. It suppresses trunk–tail mesoderm, promotes cyclopia, presumably by inhibiting formation of the prechordal plate, and induces anterior neuroectodermal structures such as brain, olfactory placodes and cement gland.

Induction of ectopic head structures

To test for more localized effects of *cerberus* mRNA, we injected it systematically into individual blastomeres at the 32-cell state[36]. In dorsal cells (B1, C1 and D1), *cerberus* mRNA resulted in severe gastrulation defects, and in animal cells (A1, A4) it induced ectopic cement glands. However, striking results were found after injection into the D4 (and to a lesser extent into C4) ventral–vegetal blastomere, which led to the formation of small ectopic head structures (Fig. 4*a*). These secondary heads were mirror duplications with respect to the anteroposterior axis, and did not contain any trunk–tail axial structures such as somites or notochord (Fig. 4*a*). In every case in which ectopic eyes developed (scored at 4 days of development), the ectopic head contained only one eye ($n = 45$), suggesting that the secondary heads lack a prechordal plate[35]. In addition, some of these animals ($n = 21$) had a secondary heart that could be seen beating at a rhythm different to that of the primary heart (Fig. 4*b*). Histological sections through the duplicated heart region (Fig. 4*c*) show that the heart consists of atrium and ventricle. Furthermore, a secondary liver (composed of sheets of basophilic hepatocytes flanked by sinusoid capillaries) is attached to the gut, and duplications in epithelial morphology (arrowheads) can be seen in the gut (Fig. 4*c*). The secondary liver arises through the formation of a second liver diverticulum, which was observed frequently in sections of stage-27 injected embryos (found in all seven embryos sectioned; not shown). Histological sections through more posterior regions (Fig. 4*d*) show that the ectopic eye has a lens and the typical retinal layered structure (Fig. 4*d*, inset). The cyclopic eye is connected to an ectopic brain containing white and grey matter, which is connected to multiple olfactory placodes (Fig. 4*d*).

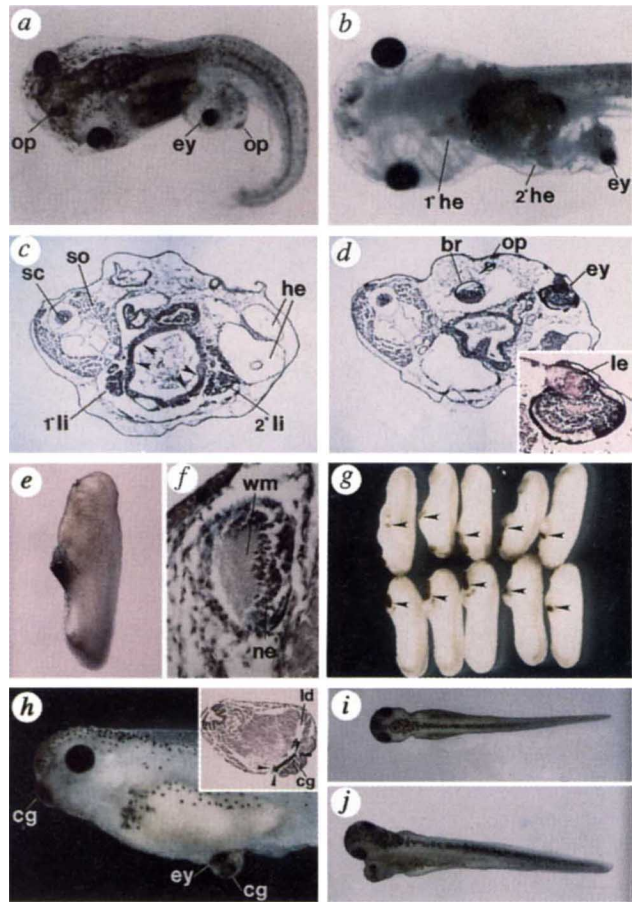

FIG. 4 Ectopic *cerberus* expression at the 32-cell stage induces head structures and duplicated heart and liver. *a*, Four-day-old embryo, anterior to the left, injected into a single D4 blastomere, showing an induced secondary head with cyclopic eye (ey) and olfactory placode (op). *b*, Ventral view of another injected embryo with ectopic head and eye (ey) and a second functional heart (2° he) containing circulating blood cells. *c*, Transverse section through the level of the ectopic heart. Note the secondary heart (he), with a ventricle and atrium as well as secondary liver (2° li) that is attached to a gut showing traces of duplicated epithelial differentiations (arrowheads); sc, spinal cord; so, somite. *d*, Transverse histological section through the level of the ectopic eye. Note the cyclopic eye (ey) and secondary brain (br) containing white and grey matter, as well as olfactory placodes (op). This particular embryo had up to eight nasal placodes. Inset, magnification of the ectopic eye, showing the typical appearance of retinal epithelium, photoreceptor cells and crystalline lens (le). *e*, Lineage-traced ectopic head structure; most *cer*-injected cells have migrated into the induced structure. *f*, Section through a lineage-labelled (*lacZ*) ectopic brain structure at day 3. Labelled cells tend to occupy the periphery of the neural tissue; wm, white matter; ne, neural. *g*, Ectopic induction of anterior structures and cement glands (arrowheads) in stage-27 embryos that were produced by transplantation into the blastocoel[7] of small animal cap fragments of *cer*-injected embryos. Control caps did not cause any induction. *h*, Ectopic head induced by transplantation of *cer*-injected animal cap cells at the gastrula stage. Note the presence of cement gland (cg) and a cyclopic eye (ey). Inset, histological section through a lineage-traced embryo at stage 27. Host cells are recruited into the cement gland (cg) and liver diverticulum (ld) and the graft (demarcated by arrowheads) is intensely labelled by the *lacZ* lineage tracer. *i*, Three-day-old embryo that received a graft of leading edge endomesoderm; no induction was found. *j*, Embryo that received a graft of more posterior endomesoderm (from the base of Brachet's cleft) where *cer* and *chd* overlap; a secondary head-like structure was formed.

METHODS. Single blastomere injections were performed in a volume of 2 nl, at a concentration of 25 ng μl^{-1} of pSP35-*cer* mRNA. Of all embryos injected ($n = 185$, 6 independent experiments) into D4 blastomeres, 75% produced ectopic patches of cement-gland tissue. Ectopic small heads with fully developed cyclopic eyes were induced at frequencies of about 35% (depending on the batch) of the embryos allowed to develop until day 4. Secondary hearts were formed in 46% of embryos with well-formed secondary heads. For the Einsteck transplantation procedure, the four animal blastomeres of 8-cell embryos were injected with 200 pg pBS-*cer* mRNA and cultured until stage 10. Animal caps were explanted and a small fragment (about $\frac{1}{4}$ of the cap) was transplanted into the blastocoelic cavity of recipient embryos at stage $10\frac{1}{2}$. For endomesoderm transplantation, transplanted cells were explanted and cultured for at least 30 min in 0.3 × Barth's to allow aggregation. Each graft filled about half of the blastocoel cavity. Histological analysis was performed as described[40].

To determine whether *cerberus* can induce ectopic structures on neighbouring cells, we co-injected *cerberus* and *lacZ* mRNAs into D4 blastomeres. The injected cells were found predominantly in the secondary head region (Fig. 4*e*), with some labelled cells trailing back towards the anus. Because the normal fate of D4 is to form posterior endoderm and mesoderm[36], the observed anterior shift suggests that *cerberus* overexpression may cause cells to migrate in the anterior direction, a change in cell behaviour that has been noted previously in *goosecoid* injections[37]. When sectioned, the labelled cells were found predominantly in the periphery of organ differentiations such as brain (Fig. 4*f*), cement gland, liver diverticulum and placode. However, some labelled cells can also contribute to all of the organs induced by *cerberus*. Although these experiments do not demonstrate a particular fate for *cerberus*-injected cells, they show that non-injected neighbouring cells are recruited into the ectopic head structures. To test whether cell recruitment can also occur at the gastrula stage, we transplanted animal caps injected with *cerberus* mRNA, together with *lacZ* mRNA as a lineage marker, into the blastocoel of stage-10 embryos (the Einsteck procedure). The transplanted cells induced head-like structures with cement glands (arrows in Fig. 4*g*) at high frequency (72%, $n = 46$, two experiments). When allowed to develop until day 4, head-like structures with cyclopic eyes were formed (Fig. 4*h*). Staining for β-galactosidase activity at stage 27 and sectioning showed that labelled grafted cells (arrowheads in Fig. 4*h* inset) were able to recruit host cells into cement gland and secondary liver diverticulum. Thus cerberus protein has non-cell-autonomous effects on the differentiation of anterior tissues.

In an attempt to test the inductive activity of the endomesoderm we transplanted the yolky cells of the leading edge of the stage-11 gastrula by the Einsteck procedure. We found that this region largely lacked inductive activity (only 2 of 42 embryos had head-like structures, two experiments). We then compared the inductive activity of the dorsal leading-edge endomesoderm with that of the more posterior endomesoderm located closer to the base of Brachet's cleft (Fig. 2*b*). Although the leading edge lacked inductive activity (Fig. 4*i*, $n = 9$), the endomesoderm just posterior to it induced head-like structures in the absence of trunk–tail differentiations (Fig. 4*j*; 8 ectopic head-like structures, 2 ectopic cement glands, $n = 18$). These observations suggest that in *Xenopus* the head organizer activity resides in the endomesoderm located at the base of Brachet's cleft, where the expression of *cerberus* overlaps with that of *chd*, *goosecoid* and *Xlim-1* (Fig. 2*b*). The lack of inductive activity of the leading edge could be affected by the experimental procedure, as the yolky explant of large cells must be allowed to aggregate for at least 30 min in saline before transplantation is possible. The interpretation we favour is that the maintenance of *cerberus* expression requires signals from the classical organizer, as suggested by the ability of *chd*, *noggin* and *follistatin* to upregulate *cerberus*, and by the lack of *cerberus* expression in ultraviolet-treated embryos (Fig. 1*d*).

The results indicate that cerberus has inductive activities on neighbouring cells, leading to the formation of ectopic heads that contain forebrain, cyclopic eyes, nasal placodes, and duplicated internal organs such as heart and liver. The *in vivo* expression of *cerberus* might be dependent on the activity of other organizer factors.

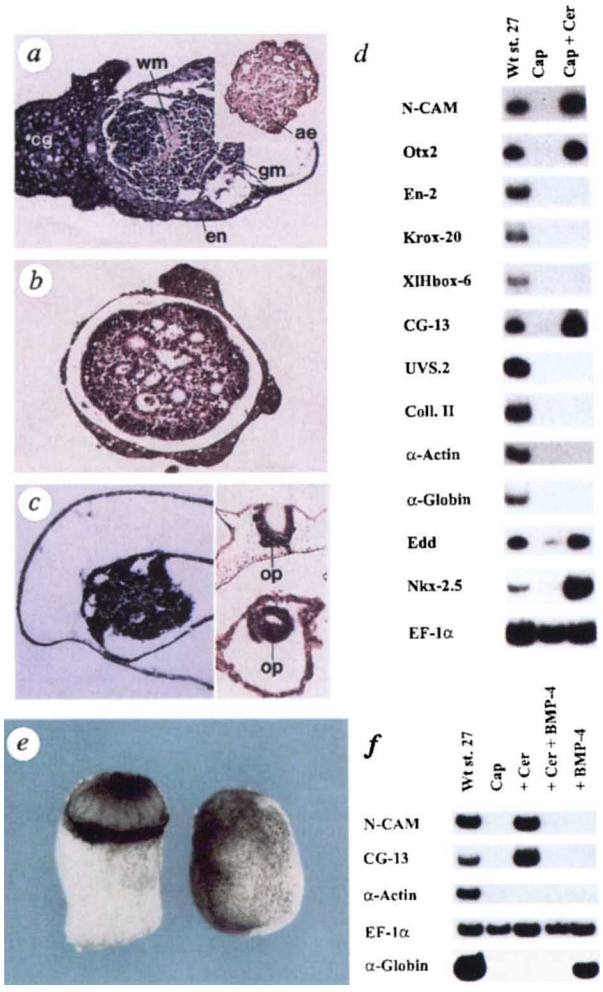

FIG. 5 *cerberus* inductions in animal cap explants. *a*, Histological section of an animal cap cultured for 4 days showing induction of brain with grey matter (dense basophilic neural cells, gm) and patches of white matter (myelinated axons, wm). Cement gland (cg) and endoderm-like cells (en) are indicated in this explant cultured for 4 days. Inset, control cap showing atypical epidermis (ae). *b*, Massive neuroepithelial differentiation of an origin difficult to determine by histological criteria. *c*, Section showing very dense neural cells that can be recognized morphologically as olfactory placodal cells. Top inset, control olfactory placode (op) of a wild-type 4-day-old embryo. Bottom inset, magnification of olfactory placode (op) induced by *cer* in an animal cap. *d*, Molecular analysis by RT–PCR of induction of anterior neural markers and other gene markers in caps injected with *cer* (see text). *e*, Embryo injected radially with 100 pg *cer* mRNA (left) or with *cer* mRNA plus 50 pg of pCSKA-*bmp-4* DNA[15] (right). Siblings were at stage 27. *f*, Molecular analysis by RT–PCR of the repression of neural and cement-gland markers by *bmp-4* in animal caps injected with *cer* mRNA. METHODS. Synthetic *cer* RNA pBS-*cer* (100 pg) was injected into each of the animal cells of 8-cell embryos. Animal caps were explanted at stage 9–10 and grown in culture until siblings reached stage 27 for molecular analyses, and for 4 days for histological sections. Conditions for RT–PCR analysis were as described[15]. Results shown are representative of several independent experiments.

Activity of *cerberus* in animal caps

As a further test of its biological activity, we injected *cerberus* mRNA into animal blastomeres of eight-cell embryos and prepared animal cap explants, which were then cultured and subjected to histological and molecular analysis for the expression of a battery of markers. Sections of *cerberus*-injected animal caps indicate a variety of neural differentiations. Control cells (Fig. 5*a*, inset) form atypical epidermis, but *cerberus*-injected caps differentiate into brain-like structures (containing clearly demarcated grey and white matter) and sometimes contain a layer of endodermal cells (Fig. 5*a*). In other cases, massive neuroepithelial differentions are formed, the histological identity of which remains unknown (Fig. 5*b*). Less frequently, explants are found that consist exclusively of dense neural vesicles and foldings that can be identified histologically as olfactory placodes (Fig. 5*c*). We have not observed such a variety of tissue patterns in neural tissue induced by *chd*[15], but in the case of *noggin* dorsoventral patterning of forebrain markers has been reported[38,39].

Molecular analysis showed that *cerberus* mRNA strongly induces a pan-neural marker (*N-CAM*) in animal caps (Fig. 5*d*). The neural tissue induced is of the anterior type, as it expresses a forebrain–midbrain marker (*Otx2*) but not more posterior markers (*En-2*, midbrain–hindbrain junction; *Krox-20*, hindbrain; *XlHbox-6*, spinal cord). A cement-gland marker (*CG-13*) is upregulated, whereas a hatching-gland marker (*USV.2*) is not induced; both organs are ectodermal derivatives. The neuralization by *cerberus* occurs in the absence of trunk mesoderm formation (*collagen II*, *α-actin* or *α-globin*). Furthermore, *cerberus* can induce the pan-endodermal marker *endodermin*[40] (*edd*), as well as high levels of an early homeobox marker for prospective heart mesoderm[34] (*Nkx-2.5*). It has been proposed that the neural inducing activities of *chd*, *noggin* and *follistatin* might be the result of antagonizing endogenous bone morphogenetic protein-4 (Bmp-4) signalling in animal cap explants[41]. To test whether Bmp-4 can override cerberus signalling, we co-injected *cerberus* mRNA and pCSKA-*bmp-4* DNA. Bmp-4 was able to counteract the morphological effects of *cerberus* radial injection (Fig. 5*e*) and the induction of *N-CAM* and a cement-gland marker in animal caps (Fig. 5*f*). Thus the antineurogenic effect of Bmp-4 is dominant over cerberus protein. This effect is not due to a shift of animal cap cells to ventral mesodermal fates because *α-globin*, which is activated by Bmp-4 alone, is repressed by co-injection of *cerberus* mRNA (Fig. 5*f*). Because Bmp-4 can counteract the effects of cerberus on ectoderm, but cerberus is dominant over the ventral mesoderm inductive activity of Bmp-4, the results suggest that cerberus and Bmp-4 signal through different pathways. We conclude that *cerberus* mRNA leads to the formation of a variety of differentiated anterior neural tissues, as well as to formation of endoderm and activation of a prospective heart mesoderm marker in animal caps.

Discussion

The cDNA *cerberus* encodes a secreted protein that is transiently expressed in a broad anterior domain of the gastrula. This domain includes the leading edge of the involuting endoderm, which, as shown here, gives rise to foregut, liver and anterior midgut. More laterally, the *cerberus* domain includes the cardiac primordia[34]. Expression of *cerberus* is excluded from the prospective prechordal plate region and from the ring of *Xbra*-expressing cells that give rise to the trunk–tail mesoderm. The biological activity of microinjected *cerberus* mRNA is congruent with this subdivision of the dorsal side of the embryo into three main regions (Fig. 2*j*). Ectopic *cerberus* mRNA inhibits prechordal plate function, leading to cyclopia, and can completely suppress formation of trunk–tail mesoderm, inhibiting notochordal, somitic and ventral mesoderm markers. Ultraviolet-ventralized embryos cannot be dorsalized by *cerberus*, which promotes anteriorization of the embryo instead. When misexpressed in a ventral–vegetal blastomere at the 32-cell stage, *cerberus* induces the formation of ectopic head structures, as well as duplications of internal organs derived from anterior endomesoderm, in particular heart and liver.

The domain of *cerberus* expression is wider than the classical Spemann organizer region defined by transplantation experiments, which occupies only 60° of the dorsal blastopore[42]. However, *cerberus* expression is dependent on the presence of a functional organizer, as ventralization by ultraviolet treatment abolishes its expression. Conversely, dorsalization by LiCl leads to radial *cerberus* expression. It is possible that *cerberus* expression

TABLE 1 *Xenopus* dorsal-specific cDNAs isolated by differential screening

Previously known genes	Gene product	No. of isolates
chordin	novel secreted protein	70
goosecoid	homeobox/transcription factor	3
pintallavis/XFKH-1	forkhead/transcription factor	2
Xnot-2	homeobox/transcription factor	1
Xlim-1	homeobox/transcription factor	1
New genes		
cerberus	novel secreted protein	11
PAPC	cadherin-like/transmembrane	2
frezzled	secreted protein	1
Sox-2	sry/transcription factor	1
Fkh-like	forkhead/transcription factor	1

Subtractive differential screening was performed essentially as described[14]. In brief, poly(A)$^+$ RNA was isolated from 300 dorsal lip and ventral marginal zone (VMZ) explants at stage $10\frac{1}{2}$. After first-strand cDNA synthesis, ~70–80% of common sequences were removed by subtraction with biotinylated VMZ poly(A)$^+$ RNA prepared from 1,500 ventral gastrula halves. For differential screening, duplicate filters (2,000 plaques per 15 cm plate; 80,000 clones screened) of an unamplified oriented dorsal lip library[46] were hybridized with radiolabelled dorsal lip or VMZ cDNA. Putative organizer-specific clones were isolated, grouped by sequence analysis from the 5′ end and whole-mount *in situ* hybridization, and classified into known and new dorsal-specific genes. Rescreening of the library (100,000 independent phages) with a *cerberus* probe resulted in the isolation of 45 additional clones; 31 were similar in size to the longest of the 11 original clones, indicating that they were presumably full-length cDNAs. The two longest cDNAs were completely sequenced.

may be maintained by diffusible signals such as chordin[14], noggin[12] or follistatin[13,15], all of which can activate its transcription in microinjected embryos. This could provide an explanation for the absence of head-inducing activity of the leading edge of the endomesoderm in the Einsteck experiments reported here, and the failure of the anterior endoderm (at a later stage) to induce cement gland and neural tissue in conjugates[43]. In both cases the inducing activity was found in more posterior regions of the endomesoderm, where the expression of *cerberus* and *chordin* overlap.

The *cerberus* mRNA is a potent neuralizing agent in injected animal caps, although we have not yet obtained purified cerberus protein to test whether this is a direct or indirect neural induction. Ectoderm is neuralized by *cerberus* mRNA in the complete absence of trunk–tail mesoderm (marked by *collagen II*, *α-actin* and *α-globin*), as is also the case for the neural inducers noggin[38], follistatin[13] and chd[15]. The panendodermal marker *endodermin* and the prospective heart mesoderm marker *Nkx-2.5* are also induced by *cerberus*. At present, therefore, we cannot determine whether cerberus protein is a direct neural inducer or whether it requires an intermediate signal from the endoderm or heart mesoderm. It has recently been reported that *chd* and *noggin*, as well as neural tissue, also induce endoderm in animal cap explants[40]. The induction of *Nkx-2.5* in animal caps has not to our knowledge been reported previously. Neuralization by *cerberus* is antagonized by Bmp-4, as is the case for *chd*, *noggin* and *follistatin*[15]. In the ectoderm, *cerberus* could act on the Bmp-4 signalling pathway or on a parallel one, with the antineurogenic activity of Bmp-4 being dominant. In the mesoderm, *cerberus* appears to act through a different signalling pathway from that of *chd* and *noggin*, because it suppresses trunk mesoderm, whereas *chd* and *noggin* are potent mesoderm dorsalizing agents[12,14].

Expression of *Nkx-2.5*, a marker for the cardiogenic region homologous to *Drosophila tinman*[34], is induced by *cerberus* mRNA, but we have been unable to detect beating hearts in explants; in intact embryos, however, functional duplicated hearts can be formed by *cerberus* injection. This suggests that in explants an additional factor may be required for overt cardiac differentiation. In *Xenopus*, there is evidence that heart induction requires at least two separate signals, one from the organizer and another from the endoderm[44,45]. The isolation of the cerberus signalling molecule now provides the opportunity to test its function in combination with signalling proteins such as chordin, noggin, follistatin, Bmp-4 and others in the genesis of organs such as heart, liver, pancreas and brain *in vitro*.

Received 28 May; accepted 1 July 1996.

1. Spemann, H. & Mangold, H. *Wilhelm Roux Arch. EntwMech. Org.* **100,** 599–638 (1924).
2. Cho, K. W. Y., Blumberg, B., Steinbeisser, H. & De Robertis, E. M. *Cell* **67,** 1111–1120 (1991).
3. Taira, M., Jamrich, M., Good, P. J. & Dawid, I. B. *Genes Dev.* **6,** 356–366 (1992).
4. Dirksen, M. L. & Jamrich, M. *Genes Dev.* **6,** 599–608 (1992).
5. Ruiz i Altaba, A. & Jessell, T. *Development* **116,** 81–93 (1992).
6. von Dassow, G., Schmidt, J. E. & Kimelman, D. *Genes Dev.* **7,** 355–366 (1993).
7. Gont, L. K., Steinbeisser, H., Blumberg, B. & De Robertis, E. M. *Development* **119,** 991–1004 (1993).
8. Lemaire, P., Garrett, N. & Gurdon, J. B. *Cell* **81,** 85–94 (1995).
9. Pannese, M. *et al. Development* **121,** 707–720 (1995).
10. Blitz, I. L. & Cho, K. W. Y. *Development* **121,** 993–1004 (1995).
11. Zaraisky, A. G. *et al. Development* **121,** 3839–3847 (1995).
12. Smith, W. C. & Harland, R. M. *Cell* **70,** 829–840 (1992).
13. Hemmati-Brivanlou, A., Kelly, O. G. & Melton, D. A. *Cell* **77,** 283–295 (1994).
14. Sasai, Y. *et al. Cell* **79,** 779–790 (1994).
15. Sasai, Y., Lu, B., Steinbeisser, H. & De Robertis, E. M. *Nature* **376,** 333–336 (1995).
16. Smith, W. C., McKendry, R., Ribisi, S. & Harland, R. M. *Cell* **82,** 37–46 (1995).
17. Jones, C. M., Kuehn, M. R., Hogan, B. L. M., Smith, J. C. & Wright, C. V. E. *Development* **121,** 3651–3662 (1995).
18. Moos, M., Wang, S. & Krinks, M. *Development* **121,** 4239–4301 (1995).
19. Vodicka, M. A. & Gerhart, J. C. *Development* **121,** 3505–3518 (1995).
20. De Robertis, E. M. *Nature* **374,** 407–408 (1995).
21. Spemann, H. *Wilhelm Roux Arch. EntwMech. Org.* **123,** 389–517 (1931).
22. Shawlot, W. & Behringer, R. R. *Nature* **374,** 425–430 (1995).
23. Acampora, D. *et al. Development* **121,** 3279–3290 (1995).
24. Kao, K. R. & Elinson, R. P. *Devl Biol.* **127,** 64–77 (1988).
25. Durston, A. J. *et al. Nature* **340,** 140–144 (1989).
26. Steinbeisser, H., De Robertis, E. M., Ku, M., Kessler, D. S. & Melton, D. A. *Development* **118,** 499–507 (1993).
27. Harland, R. M. *Meth. Cell Biol.* **36,** 685–695 (1991).
28. Nieuwkoop, P. D. & Florschütz, P. A. *Archs Biol., Paris* **61,** 113–150 (1950).
29. Pasteels, J. *Archs Biol., Paris* **60,** 235–250 (1949).
30. Keller, R. *Meth. Cell Biol.* **36,** 61–113 (1991).
31. Smith, J. C., Price, B. M. J., Green, J. B. A., Weigel, D. & Herrmann, B. G. *Cell* **67,** 79–87 (1991).
32. Holtfreter, J. *Wilhelm Roux Arch. EntwMech. Org.* **138,** 522–738 (1938).
33. Hausen, P. & Riebesell, M. *The Early development of Xenopus laevis* (Springer, Berlin, 1991).
34. Tonissen, K. F., Drysdale, T. A., Lints, T. J., Harvey, R. P. & Krieg, P. A. *Devl Biol.* **162,** 325–328 (1994).
35. Adelman, H. B. *Q. Rev. Biol.* **11,** 284–304 (1936).
36. Dale, L. & Slack, J. M. W. *Development* **99,** 527–551 (1987).
37. Niehrs, C., Keller, R., Cho, K. W. Y. & De Robertis, E. M. *Cell* **72,** 491–503 (1993).
38. Lamb, T. M. *et al. Science* **262,** 713–178 (1993).
39. Knecht, A. K., Good, P. J., Dawid, I. B. & Harland, R. M. *Development* **121,** 1927–1936 (1995).
40. Sasai, Y., Lu, B., Piccolo, S. & De Robertis, E. M. *EMBO J.* (in the press).
41. De Robertis, E. M. & Sasai, Y. *Nature* **380,** 37–51 (1996).
42. Gerhart, J. *et al. Development* **107** (suppl.), 37–51 (1989).
43. Sive, H. L., Hattori, K. & Weintraub, H. *Cell* **58,** 170–180 (1989).
44. Sater, A. K. & Jacobson, A. G. *Development* **108,** 461–470 (1990).
45. Nascone, N. & Mercola, M. *Development* **121,** 515–523 (1995).
46. Blumberg, B., Wright, C. V. E., De Robertis, E. M. & Cho, K. W. Y. *Science* **253,** 194–196 (1991).
47. Ozaki, T. & Sakiyama, S. *Proc. natn. Acad. Sci. U.S.A.* **90,** 2593–2597 (1993).
48. Jowett, T. & Lettice, L. *Trends Genet.* **10,** 73–74 (1994).

ACKNOWLEDGEMENTS. We thank J. Gerhart for insights about cell fates in the *Xenopus* gastrula; L. Leyns, S. Piccolo and D. Bachiller for reviewing the manuscript; A. Cuellar and L. Tabata for technical assistance; and A. De Robertis for preparing the manuscript. T.B. was an EMBO fellow and is now an HFSPO fellow. This work was supported by a grant from the NIH and the Norman Sprague Endowment. E.M.D.R. is a Howard Hughes Medical Institute investigator.

CORRESPONDENCE and requests for materials should be addressed to E.M.D.R. The *cerberus* cDNA sequence has been deposited in GenBank database, accession no. U64831.